T-Cell Activation: A Queuing Theory Analysis at Low Agonist Density

J. R. Wedagedera* and N. J. Burroughs†
*Department of Mathematics, University of Ruhuna, Matara, Sri Lanka; and †Mathematics Institute, University of Warwick, Coventry, United Kingdom

ABSTRACT We analyze a simple linear triggering model of the T-cell receptor (TCR) within the framework of queuing theory, in which TCRs enter the queue upon full activation and exit by downregulation. We fit our model to four experimentally characterized threshold activation criteria and analyze their specificity and sensitivity: the initial calcium spike, cytotoxicity, immunological synapse formation, and cytokine secretion. Specificity characteristics improve as the time window for detection increases, saturating for time periods on the timescale of downregulation; thus, the calcium spike (30 s) has low specificity but a sensitivity to single-peptide MHC ligands, while the cytokine threshold (1 h) can distinguish ligands with a 30% variation in the complex lifetime. However, a robustness analysis shows that these properties are degraded when the queue parameters are subject to variation—for example, under stochasticity in the ligand number in the cell-cell interface and population variation in the cellular threshold. A time integration of the queue over a period of hours is shown to be able to control parameter noise efficiently for realistic parameter values when integrated over sufficiently long time periods (hours), the discrimination characteristics being determined by the TCR signal cascade kinetics (a kinetic proofreading scheme). Therefore, through a combination of thresholds and signal integration, a T cell can be responsive to low ligand density and specific to agonist quality. We suggest that multiple threshold mechanisms are employed to establish the conditions for efficient signal integration, i.e., coordinate the formation of a stable contact interface.

INTRODUCTION

Immune responses rely upon the detection of specific antigens by T cells, antigen exposure activating a T cell which possibly leads to cell proliferation and differentiation. The activation process is complex and multifaceted, and despite decades of research remains controversial. The complexity of T-cell activation and the associated diversity of activation criterion utilized for quantification have made consensus illusive. Key issues are the mechanisms that produce an activation process that is both specific to particular antigens and sensitive down to single copies of a ligand, and the spatial-temporal requirements for activation. A hierarchy of events can be distinguished during the process of activation. Initially the T cell comes into surface contact with another cell where the T-cell receptor (TCR) may interact with its ligand (peptide-MHC; i.e., pMHC). Then TCR binding to its specific ligand leads to phosphorylation of the receptor and recruitment of adaptors and kinases that comprise the signaling cascade. The next level of signaling is the integration of these signals to ultimately determine cell function; this includes regulation of the cytoskeleton, control of adhesion within the cell-cell contact (1), directed secretion at the interface (2), and gene transcription. Appropriate gene activation is the hallmark of cell activation, specifically cytokine production (e.g., interleukin-2 (IL2) and interferon gamma (IFNγ)), and expression of activation markers such as CD69, and cytokine receptors such as the IL2 receptor. Activation may ultimately result in cell cycle progression through cytokine-mediated proliferation.

Thresholds have remained the predominant means of analysis of this activation/signaling sequence, i.e., a T cell becomes activated (as measured by function X) if the stimulus is above a threshold. In practice, a hierarchy of thresholds is observed for different cell responses (3–5), with good consistency between cells for the relative threshold order:

$$Cytotoxicity \ll Cytokine\ production < Cell\ proliferation.$$

However, these thresholds depend on the stimulus conditions, the most significant change occurring in the presence of co-stimulation through co-receptors such as CD28 (6). The threshold concept received recent support from single molecule studies where thresholds in the range of 1–10 agonist pMHCs were observed (7), significantly lower than previously reported. However, recent experimental data suggests that T-cell activation is not achieved in a single step or commitment event, but is a multistep sequence of events in which disruption of signaling proportionally reduces activation (8,9). This quantitative dependence on the temporal sequence of events has been observed in other studies, T-cell survival and proliferation correlating with duration of antigen exposure (10–12), while T cells can be activated by a series of transient short-lived cell encounters (13). This temporal dependence supports an earlier hypothesis that a T cell effectively counts the number of productive TCR/pMHC interactions, a conclusion originally based on the high correlation of cell response to the fraction of downregulated TCRs (14).

In this article we consider simple activation models motivated by the dependence of activation on the temporal aspects of the signal. Our aim is to provide a framework for the analysis of TCR triggering, incorporating, in our opinion, the vital components of stochasticity and signal history, and

Submitted May 17, 2005, and accepted for publication April 17, 2006.

Address reprint requests to N. J. Burroughs, E-mail: njb@maths.warwick.ac.uk.

0006-3495/06/09/1604/15 $2.00

doi: 10.1529/biophysj.105.066001

clarifying the limitations of simple models in explaining T-cell activation characteristics. We define threshold and signal integration models, and analyze their specificity and sensitivity. Given the complexity of the activation process our models do not address all aspects of activation; we ignore spatial effects, nonlinearity, and feedback. Our philosophy is to understand the shortcomings of the simplest system to elucidate the determinants of signal detection characteristics. We base our models on queuing theory; a TCR enters the queue upon full activation and exits by downregulation or inactivation. This formulation directly accounts for the noise associated with signaling based on a finite number of signaling molecules. We use this model to analyze various activation criteria reported in the literature.

Although T-cell activation has been a fertile area for mathematical modeling there have been very few studies that include system stochasticity (15–19), and none that have explored the consequences of low agonist density on signaling characteristics. Conceptually, kinetic proofreading has been a key platform on which to discuss specificity (20,21), although this was recently criticized for being insufficiently sensitive at high specificity (22). Despite these and other T-cell activation models, theoretically it remains unclear how complex TCR triggering dynamics must be to filter out self-peptide noise while achieving high sensitivity, and further, the circuit architecture that is required, e.g., strength of nonlinear feedback (23,24), filtering, or amplification steps. This contrasts to the Fc receptor where theoretical understanding is further advanced and limiting factors can be assessed at the model level (25).

T-CELL SIGNALING: A SEQUENCE OF EVENTS

T-cell activation involves a complex series of spatial and temporal events over three timescales: early (seconds); cell and receptor reorganization (minutes); and gene activation (hours). These are enumerated as follows:

Migration stop signal

On first contact with an antigen-presenting cell (APC), a T cell must be triggered to stop migrating. This stop-signal is antigen-specific, 8% of cells stopping in absence of agonist, 95% stopping when 1–10 pMHCs were in the interface (CD4 cells with B cell lymphoma APCs (26)). This initial agonist-dependent signal probably invokes upregulation of adhesion receptors such as LFA-1. Dendritic cells are an exception, T cells displaying an interest even in absence of agonist (27), which is probably related to the antigen-independent adhesion processes observed in these cells.

Calcium spikes and sustained signals

One of the earliest signals is a calcium rise, observed even with a single pMHC in the interface (26). Calcium signals are quantal, with the 4 min (and 10 min) integrated signal rising linearly with pMHC over the range of 1–10 pMHCs, saturating at >20 pMHCs (cytotoxic T cells (7)), >10 pMHC (T helper cells (26)). T-cell activation has an absolute requirement for extracellular calcium; specifically, calcium levels must remain above 400 nM for at least 2 h during cell stimulation for activation (28,29). However, spike dynamics and sustained calcium levels are likely controlled by different mechanisms (30).

Cell polarization

Within minutes of APC contact, the T cell reorients toward the APC/target cell; specifically, actin accumulates at the interface and the microtubule organizing center localizes near the interface (31).

Synapse formation

Within the T cell-APC interface, a macroscopic patternation is established over 3–10 min, with TCR/pMHC in the center surrounded by adhesion molecules ICAM-1/LFA-1 (32). This patternation requires ≥ 10 pMHC agonists within the contact interface (7,26). Before synapse maturation, TCR clusters are observed at 50 s and correlate with high levels of kinase activation (33,34), while CD8β and AKT (indicative of phosphoinositol PIP_3) aggregation occurs at the interface within 1 min (7).

Gene transcription

The sequence of events at the molecular level is well established for a few transcription factors; for example, NFκB translocates to the nucleus when the inhibitor IκB is destroyed on T-cell ligation (35). Elevated calcium is required to prevent accumulation of the inhibitor and retain the transcription factor in the nucleus (36), thereby underpinning the requirement for continual signaling for gene transcription.

Deconjugation

The natural termination of signaling and breakup of T cell-APC conjugates is poorly understood. TCR triggering may fall below the level required to sustain conjugation through TCR downregulation or inhibition of signaling by SHP-1 recruitment (37). However, the cell environment may also play a role, since, in three-dimensional lattices, APC interactions were transient and short-lived, with an average of 6–12 min (13)—similar to the interactions observed in vivo, indicating that a competing balance of signals may determine T-cell dynamics (38). Despite these inconsistencies, most reports agree that activation of naive T cells takes 10–24 h.

It is clear that there are multiple levels of information extraction over a range of timescales in the T cell-APC

interaction. Initial signals (e.g., indicated by cytosolic calcium levels) must reach sufficient levels to initiate formation of a cell conjugate, with a series of later additional thresholds to establish, for example, a synapse. There is an absolute requirement for continued signaling (6); TCR triggering in the T cell-APC interface is required to maintain the synapse since interruption of antigen ligation results in loss of synaptic patterning (the ICAM-1 annulus), with a decay of calcium and kinase (PI3K) activity (9). If kinase activity is interrupted synapse organization is also destroyed (CD2 aggregation as the observable under PP2 treatment (8)). These studies demonstrate that TCR triggering continues within the synapse even though the TCR density had decreased by downregulation and continued signaling is essential for activation. Of particular importance is the approximate linearity of the T-cell response with duration of signaling; specifically, cytokine production is linear in the total period of antigen exposure and intermittent interruption of signaling can be compensated by lengthening the time of exposure (8). In these studies, signal mediators, such as calcium levels, decayed within a minute of signaling interruption. T-cell activation is therefore a sequence of events, earlier events such as the calcium elevation and synapse formation probably being required but not committing the T cell to activation or to particular cell functions—functions that are further regulated through a series of thresholds or checkpoints either in parallel, or in a sequential hierarchy (3–5).

BASIC QUEUING MODEL AND THE CRITERIA FOR ACTIVATION

In this section we present a queuing theory model for the number of fully activated TCRs. The generation of fully activated TCRs is modeled by a kinetic proofreading (KPR) scheme (20,21), which we discuss in the deterministic formulation. A threshold strategy is defined for the queuing model as a crossing time for the (Erlang) queue, which is solved using a Markov-chain approach. We approximate the queue with a stochastic differential equation that provides an analytical treatment of the stationary queue and is utilized in the analysis of the time-integrated signal.

Initiating TCR signaling: a kinetic proofreading scheme

We utilize a kinetic proofreading scheme (20,39), with $m + 1$ steps for the activation of TCRs (see Fig. 1), steps which can correspond to TCR phosphorylation or recruitment and activation of key kinases and adaptors (40). TCRs (denoted by T) bind with pMHC with forward rate k_{on} and backward rate k_{off}, independent of the activation state of the TCR. Fully activated TCR/pMHC complexes are denoted as C^*, and intermediate levels of activation as C_k. Activated TCR/pMHC complexes dissociate with rate k_{off} into a signaling TCR denoted by T^*, which are endocytosed/downregulated with rate μ (Fig. 1). Inactivation can also be included as a distinct process from downregulation returning TCRs to the inactive pool, $T^* \rightarrow T$ (41); then μ, now the combined rate, is increased compared to the value used here. Downregulation is assumed slow, therefore a pseudo-equilibrium is established for the complex densities (20)

$$C_0 = \frac{k_{on} TM}{k + k_{off}},\ C_r = \left(\frac{1}{1 + \frac{k_{off}}{k}}\right)^r C_0 = \alpha^r C_0, r = 1, 2..m, \quad (1)$$

where $\alpha \equiv \alpha(k_{off}) = 1/(1 + k_{off}/k)$. The pseudo-equilibrium approximation for C^* is $C^* = (k/k_{off})\, C_m = (k/k_{off})\, \alpha^m C_0$. Under changes in the KPR scheme length m, we rescale the rate of progression k to preserve the average time to reach the final state, conditional on not unbinding from the ligand, i.e., $k = \beta\ (m + 1)$ with $\beta = (k_{off})_{opt} = 0.1\ s^{-1}$ the optimal off-rate for a TCR/pMHC interaction.

The total number of pMHC complexes M_{total} is assumed conserved for simplicity. This will be valid at short times and once the synapse is formed since pMHC are trapped in the center of the contact interface (42). There is a similar conservation for the number of TCRs within the pseudo-equilibrium approximation, which fails to hold on the downregulation timescale under large agonist densities since $(d/dt)(T + \sum_{i=0}^{m} C_i + C^* + T^*) = -\mu T^*$; however, TCR numbers normally exceed the number of agonists (pMHC) by an order of magnitude. In our applications the number of agonist pMHC (1–1000) is low and thus the number of TCRs (10,000–30,000) on the surface can be considered in excess. Thus, TCR loss is negligible and the free TCR density (R) can be approximated by the total TCR density to a good approximation.

The pseudo-equilibrium solution determines the expected number of complex molecules in each compartment and the intercompartment flow. We define the triggering rate λ as the flow of molecules into the fully activated class $C_m \rightarrow C^*$. In practice, the partially activated TCRs in the KPR scheme will rapidly equilibrate and fully activated TCRs accumulate as unbound T^*; thus, at equilibrium, the triggering rate is equal to the flow $C^* \xrightarrow{k_{off}} T^*$, giving (valid for $m \geq 0$)

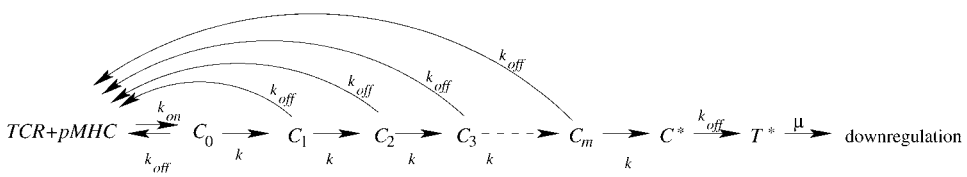

FIGURE 1 Schematic for the kinetic proofreading scheme (KPR).

$$\lambda = k_{\mathrm{off}} C^* = \alpha^{\mathrm{m}} k C_0 = \frac{\beta(m+1)\alpha^{\mathrm{m}} M_{\mathrm{total}}}{\dfrac{\mathrm{k_{off}}}{\alpha \mathrm{k_{on}} \mathrm{T}} + \dfrac{1-\alpha^{\mathrm{m}+1}}{1-\alpha} + \dfrac{\beta(\mathrm{m}+1)\alpha^{\mathrm{m}}}{\mathrm{k_{off}}}}. \tag{2}$$

Note that if $k_{\mathrm{off}} \to \infty$, the triggering rate decays to zero as $\beta(1+m)k_{\mathrm{on}} T M_{\mathrm{total}} k^{\mathrm{m}+1} k_{\mathrm{off}}^{-2-m}$.

Modeling triggered TCRs as a queue

Each compartment C_{k} in the KPR scheme can be considered as a queue. These are Poisson queues with Poisson input, and thus the output process C_{k} to $C_{\mathrm{k}+1}$ is also Poisson (total exit rate is $(k_{\mathrm{on}} + k_{\mathrm{off}})E[\mathrm{C_k}]$ at stationarity and a probability α of progression). Thus, the free TCR queue T^* is therefore a Poisson queue,

$$\xrightarrow{\lambda = \mathrm{k_{off}} C^*} \boxed{\mathrm{T^*(t)}} \xrightarrow{\mu \mathrm{T}*(\mathrm{t})} \text{downregulation},$$

or a jump Markov process comprising two independent Poisson processes with rates $\lambda = k_{\mathrm{off}}\mathbb{E}[C^*]$ and $\mu T^*(t)$ and jumps of size +1 and –1, respectively.

We define a threshold condition for cell activation with signaling threshold n as the requirement that the number of fully activated TCRs must exceed n within a (given) time interval τ, i.e., $T^*(t) > n$ at some time $t < \tau$. In terms of the queue, the probability of activation is

$$\mathbb{P}\left[T^*(t) < n \text{ for } t < t', T^*(t') = n | T^*(0) = 0, 0 < t' < \tau\right]. \tag{3}$$

This probability is the first crossing probability for level n where crossing is required to occur within time τ. First crossing times can be analyzed with Markov chains and approximated using large deviation theory.

To simplify our analysis, we restrict ourselves to enumerating only the free fully activated TCRs (i.e., we ignore the contribution from the C^* compartments, which are also fully competent at signaling since $\mu \ll k_{\mathrm{off}}$ and thus $C^*(t)$ is a minor population, $C^*(t) \ll T(t)$). We also assume that TCRs are in excess and thus the pool-size of free TCRs is constant (even though TCRs are held within compartments C_{k} and C^*, and are downregulated). These assumptions can be dropped, but complicate the exact analysis. Note that our queue counts an absolute number of activated TCRs T^*, which contrasts to the free TCR pool-size enumerated as a density R.

Exact Markov-chain computation for threshold strategies

We are interested in estimating the probability of reaching the threshold n starting from an initial level of 0 (Eq. 3). Since the process $T^*(t)$ is a continuous-time Markov process, with $T^*(0) = 0$, and $T^*(t) = n$ for some $t \le \tau$, we construct the Markov chain with states $k = 0, 1, \ldots, n–1, n$ and define the probabilities $p_{\mathrm{k}}(t)$ of occupancy of state k at time t. Denote by $\mathbf{p}(t) = (p_0(t), p_1(t), \ldots, p_{\mathrm{n}}(t))$, the probability vector of state occupancy at time t, then the transition dynamics is given by $d\mathbf{p}/dt = \mathbf{p}G$, where the generator matrix $\mathbf{G}$ is given by

$$G = \begin{pmatrix} -\lambda & \lambda & 0 & \cdots & & & & 0 \\ \mu & -(\lambda+\mu) & \lambda & 0 & \cdots & & & 0 \\ 0 & 2\mu & -(\lambda+2\mu) & \lambda & 0 & \cdots & & 0 \\ \vdots & & & & & & & \\ 0 & \cdots & 0 & k\mu & -(\lambda+k\mu) & \lambda & 0 \cdots 0 & \\ \vdots & & & & & & & \\ 0 & \cdots & & & & 0 & 0 & 0 \end{pmatrix}. \tag{4}$$

Note that the final state is now a sink, since we are computing a crossing time. In the threshold strategy, we are interested in calculating $\mathbb{P}[T^*(t) \ge n \text{ for any } t \le \tau]$. At time $t = 0$ we have $\mathbf{p}(0) = (1, 0, \ldots, 0)$ and at time $t > 0$,

$$\mathbf{p}(t) = \mathbf{p}(0)e^{Gt}. \tag{5}$$

The desired probability $\mathbb{P}_{\mathrm{act}}(\tau, \lambda, n) = \mathbb{P}[T^*(t) \ge n \text{ at some } t < \tau] = p_{\mathrm{n}}(\tau)$. This is a function of the time-interval τ and the triggering-rate λ (Eq. 2), which is itself a function of agonist density M_{total} and agonist quality, predominantly k_{off}. In fact we determine the threshold n in Results by fitting the probability $\mathbb{P}_{\mathrm{act}}$ to a number of specific experimentally observed values described in Table 1.

A stochastic differential equation model

The queue model can be approximated by a stochastic differential equation (sDE), an approximation that improves as the equilibrium queue size increases. Let $T^*(t) \in \mathbf{R}$ be the number of triggered TCRs in the queue, now a continuous random variable, then the dynamics is given by $dT^* = (\lambda - \mu T^*)dt + \sigma(T^*)dW$, where $W(t)$ is a Weiner noise and $\sigma(T^*)$ is the standard deviation of the process. To fit parameters we match the variance with that of the queue. For a time-interval Δt, $var_{\mathrm{queue}}(\Delta T^*) = var(\text{input}) + var(\text{output}) =$

TABLE 1 Parameter values used to match experimentally observed activation probabilities with optimal agonists, dissociation rate $k_{off} = 0.1\ s^{-1}$, and with $m = 7$ activation reactions (see Basic queing model and the criteria for activation)

Label	Time τ	M (# pMHC)	Threshold*	$\mathbb{P}_{act}$ at $k_{off} = 0.1\ s^{-1}$†	Equilibrium	Remarks
Ca	30 s	2	1	0.86 (0.95)	22	(26)
Calcium signals sustained on 2 pMHC, 95% of cells stop migrating. Calcium peaks at 30–60 s.						
Cx	10 min	3	25	0.8 (5/6)	33	(7)
Cytotoxicity (2C cells) observed after 5–15 min: 1/9 cases at 2 pMHC, 5/6 cases at 3 pMHC.						
IS	30 s	10	6	0.91 (0.90)	108	(7,34)
Synapse formation with 10 pMHC in ~90% of cases, early TCR clusters seen by 50 s.						
Cy	3 h	100	1172	0.50 (0.50)	1082	(52)
IFNγ secretion, 100 nM pulsing (~100 pMHC) gives 50% of maximum signal.						
B	10 min	10	83	0.9	108	IS comparison
C	1 h	10	121	0.9	108	IS comparison
D	10 min	100	908	0.5	1082	Cy comparison
E	1 h	100	1147	0.5	1082	Cy comparison

*Computed from Eq. 5 to the nearest integer.
†Value in parentheses is estimated from the cited study.

$\lambda\Delta t + \mu T^*\Delta t$; thus equating this to the variance of the sDE, we obtain $\sigma^2 = \lambda + \mu T^*(t)$.

The expected queue size $\mathbb{E}[T^*]$ satisfies the differential equation $d\,\mathbb{E}[T^*]/dt = \lambda - \mu\mathbb{E}[T^*]$; i.e., there is an exponential approach to the stationary (equilibrium) level $\rho = \lambda/\mu$. Our interest is in fluctuations around the stationary equilibrium, so we simplify the sDE. Define $X(t) = T^* - \rho$, then

$$dX = -\mu X(t)dt + \sigma dW(t), \sigma = (2\lambda)^{\frac{1}{2}}, \tag{6}$$

where we ignore dependence of the noise σ on the state, valid if fluctuations $X(t)$ are small relative to ρ. This is, in fact, the Ornstein-Uhlenbeck process for which the exact solution is given by

$$X(t) = X(t_0)\exp[-\mu(t-t_0)] + (2\lambda)^{\frac{1}{2}}\int_{t_0}^{t}\exp[-\mu(t-s)]dW(s), \tag{7}$$

i.e., $X(t)$ is a sum of Gaussians ($X(t_0)$ fixed or drawn from a Gaussian), and therefore $X(t)$ is normally distributed with mean and variance,

$$\mathbb{E}[X(t)] = \exp[-\mu(t-t_0)]\mathbb{E}[X_0],$$
$$var[X(t)] = \exp[-2\mu(t-t_0)]\left(var(X_0) - \frac{\sigma^2}{2\mu}\right) + \frac{\sigma^2}{2\mu}.$$

In particular, when $X(t)$ is stationary, i.e., when $t_0 \to -\infty$, we find $\mathbb{E}[X] \to 0$ and $var(X) \to \sigma^2/2\mu$.

Time-integrated signals: quantifying responses in the stationary queue

To quantify T-cell responses under an integrated signal, define the functional

$$a(\tau) = \int_0^\tau T^*(t)dt \tag{8}$$

as a measure of the signal strength over the duration of time τ. For example, a triggered TCR T^* acts as a source of activated signaling mediators throughout its lifetime. This measure of signal strength will be appropriate provided there are no limiting factors down-stream. More generally we could use $\hat{a}(\tau) = \int_0^\tau (T^*(t)/(K+T^*(t))dt$ if there is a limiting factor with a saturation level K, e.g., Lck limitation (43). Most of our analysis is with low levels of agonist, and thus we assume saturation does not occur.

We wish to compute $\mathbb{E}[a(\tau)]$ and $var[a(\tau)]$ for the system while at stationarity. For the Ornstein-Uhlenbeck process, $a(\tau)$ is Gaussian with

$$\mathbb{E}[a(\tau)] = \rho\tau = \frac{\lambda}{\mu}\tau,$$
$$var[a(\tau)] = 2\iint_{s>u}^{\tau}\mathbb{E}[X(s)X(u)]dsdu = \frac{\sigma^2}{\mu^3}(\mu\tau + \exp[-\mu\tau] - 1). \tag{9}$$

For large τ we have $var[a(\tau)] \approx \sigma^2\tau/\mu^2 \approx 2\lambda\tau/\mu^2$. This gives an estimate for the relative error as $\sqrt{2/\lambda\tau}$; in particular, the error is reduced for a given triggering rate by extending the time interval. For triggering rates of 0.4 per second, e.g., an optimal agonist at density $M_{total} \approx 10$ in the contact interface, a relative error of 2% is achieved over a time interval of 5 h.

Incorporating TCR downregulation

Over extended periods at high agonist density, TCR downregulation can have a significant impact on signal strength and thus needs to be incorporated in signal-integration models. To model TCR downregulation kinetics, let W be the production rate of TCRs to the cell surface per second, μ_0 be the constitutive rate of loss of TCRs from the cell surface per second, and μ_d be the rate of triggered TCR endocytosis

(triggered TCRs being destroyed (44)). Thus, we are not explicitly modeling TCR recycling (45). We have dynamics

$$\frac{dR}{dt} = W - \mu_d \frac{T^*}{A} - \mu_0 R, \tag{10}$$

where we introduced the area of the cell $A \sim 300\ \mu m^2$, since R is a density while the queue is an absolute count of triggered TCRs. When there is no ligand, i.e., $T^* = 0$, we have a steady state given by $R_{ss,0} = W/\mu_0$. When agonist is present, the surface TCR density decreases with an equilibrium given by the quadratic $W - \lambda(k_{off}, R, M)A^{-1} - \mu_0 R = 0$, setting $\mu_d T^* = \lambda$. The new steady state is, using the triggering-rate expression Eq. 2,

$$R = \frac{1}{2\mu_0 c}[-a + cW - b\mu_0 + \{(cW + b\mu_0)^2 - 2a(cW - b\mu_0) + a^2\}^{1/2}], \tag{11}$$

where $a = \alpha^m k M_{total}/A$, $b = (k + k_{off})/k_{on}$, and $c = (1 - \alpha^m)/(1 - \alpha) + k\alpha^m/k_{off}$. Steady-state TCR densities are shown in Fig. 2 under differing levels of agonist density and quality (k_{off}); in particular, at low levels of agonist ($M_{tot} < 1000$), downregulation can be ignored. The positive root is the only physical solution. Linearization in M_{total} gives $R \sim R_{ss,0} - aW/(\mu_0(cW + \mu_0 b))$.

More complex models for downregulation have been presented elsewhere (41,46).

RESULTS

Fitting activation strategies

To assess the relative merits of thresholds set over different periods of the activation process, we define a number of activation strategies based on experimentally determined conditions. These encompass both early and late decisions. A threshold strategy for a particular cell response consists of a commitment timescale τ for the cell response and the probability of activation of that response at a given agonist concentration within that time τ. Specific strategies, with identifying labels used throughout this article, are as follows (see Table 1):

Ca. . .Calcium threshold with a time window $\tau = 30$ s. This is the initial interest signal to strengthen the contact, the cell moving on without this signal.

Cx. . .Cytotoxic response, i.e., cell-killing (CD8 T cells), which occurs on a timescale of 5–15 min with high sensitivity.

IS. . .Immunological synapse formation, or the formation of a macroscopic receptor patterning in the T cell-APC contact interface, initial reorganization being visible by 50 s of contact.

Cy. . .Cytokine secretion, requiring gene transcription, and which occurs on a scale of hours.

For example, during the initial contact of a T cell with an APC, there is a competition between continuation of peptide-scanning on the cell surface and signals to move-on. The latter signals possibly derive from the extracellular matrix since artificial three-dimensional matrix studies observed short scanning times of mean duration 6–12 min, independent of agonist (13). Thus, if sufficient stimulus is received from the APC, the cell will strengthen its adhesive contact and enlarge the area of contact, e.g., through LFA-1 affinity upregulation (47), and orient toward the APC. This initial interest signal we encompass in the calcium threshold condition *Ca* (see Table 1), simplifying the analysis to a set time-interval τ instead of the competition of signals implied above, where τ would be exponentially distributed. Because these strategies vary in the cell threshold n, activation probability $\mathbb{P}_{act}$, and time-interval τ, we supplement these with additional sets, *B–E* (see Table 1), to provide a basis to assess the effect of the various parameter changes.

Mathematical fitting of an activation strategy requires us to determine the activated TCR threshold n given the activation probability $\mathbb{P}_{act}$ under the specified conditions, i.e., using Eq. 5. In general, this threshold is low for short time-windows and low agonist-density M_{total}, and increases as τ or M are increased; i.e., we need more activated TCRs to match the given activation probability (Table 1). Further, the threshold n is not necessarily less than the queue equilibrium level ρ.

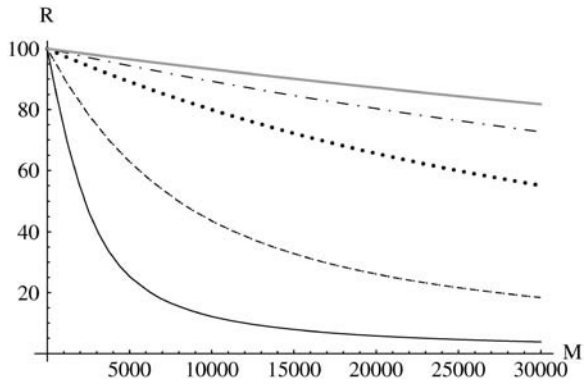

FIGURE 2 Equilibrium TCR surface density (mol μm^{-2}) as a function of agonist numbers M in the interface. Cases shown are $k_{off} = 0.01$, 0.1, 0.4, 0.7, and 1.0 s^{-1}, with less downregulation as k_{off} deviates further from the optimal off-rate $\approx 0.1\ s^{-1}$.

Activation probabilities

Kinetic proofreading scheme length

To determine an appropriate length for the kinetic proofreading scheme (see Fig. 1), we examined the triggering rate as a function of off-rate k_{off} with different numbers of intermediate steps m, rescaling the transition rate $k \propto m + 1$ to preserve sensitivity. This differs from the study of Chan et al. (22), who analyzed an unconstrained system—thus explaining our differing conclusions. Although the triggering rate was

maximal at $\sim k_{off} = 0.1$–$0.2\ s^{-1}$ for all m, the triggering rate becomes more concentrated around the optimum as m increases (Fig. 3 *A*). When there are no intermediate steps, the triggering rate had a weak dependence on k_{off}, and above $m = 3$ there is little dependence on m. Because of the rescaling of the transition rate k with m, the sensitivity and specificity converge as $m \to \infty$; the probability of an agonist to become fully activated converges to $e^{-k_{off}/\beta}$, or ~ 0.37 for an optimal agonist. The specificity can be quantified in terms of the elasticity $(\partial log \mathbf{P}_{act})/(\partial log\, k_{off}) = -(k_{off}/\beta)$ (evaluated for $m \to \infty$), indicating a log-per-log relative change in the specificity for an optimal agonist, i.e., $\Delta \mathbf{P}_{act}/\mathbf{P}_{act} \approx -\Delta k_{off}/k_{off}$. We use $m = 7$ in the following, although all $m > 3$ had similar behavior (data not shown). The triggering rate increases in M_{total} (in fact, linearly) as indicated by Eq. 2. This highlights the interplay between agonist quality and agonist density in all kinetic proofreading schemes; poor agonist quality can be compensated for by a higher density of agonist, i.e., there is a continuum of $\{M_{total}, k_{off}\}$ giving the same triggering rate (Fig. 3 *C*) and thus activation characteristics.

Queue dynamics

We initiate the queue at $t = 0$ (first contact) with $T^* = 0$. The queue then fills with approximately linear kinetics before settling at an equilibrium level (Fig. 4). Since the down-regulation rate is slow, a fully activated TCR has an average lifetime of 5 min (μ^{-1}), and thus contributes to signaling for that period of time. This timescale determines the approach to equilibrium, $\mathbb{E}[T^*(t)] = \lambda(1 - e^{-\mu t})/\mu$, i.e., at 10 min, it is within 17% of the equilibrium value (Fig. 4). This means that for time intervals $\tau <\sim 5$ min, the queue size is effectively the count of the number of triggering events. This is what distinguishes the behavior between time intervals of 30 s and 5 min with $\geq$10 min; once the queue has reached equilibrium the queue no longer counts productive triggerings. Thus, we expect large behavioral differences between 30-s and 10-min time intervals, but much less between 10 min, 1 h, and 10 h because, in the latter, the queue is effectively stationary. This is clear from the differences between the threshold and equilibrium values for the various conditions (see Table 1); at short times the thresholds are very low, much lower than the steady-state queue size. This is because the threshold is implemented on the rising phase of the queue.

Specificity at given agonist density M

Of key importance to T-cell activation is the sensitivity of the system to small numbers of agonist peptides and the specificity of the system to ligand quality; for T cells, the primary determinant of activation, or measure of ligand quality, is the TCR/pMHC off-rate, k_{off} (48).

The ability to discriminate agonist quality (k_{off}) varies significantly between the activation strategies of Table 1; the

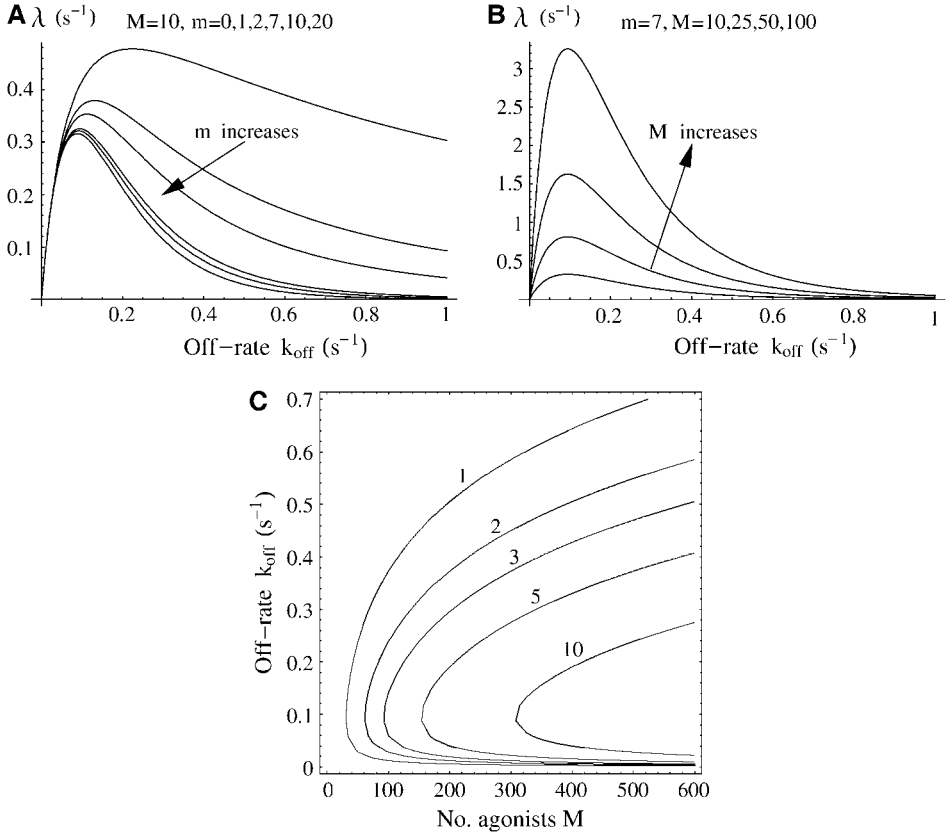

FIGURE 3 Triggering rate λ dependence on agonist density M and KPR scheme length m. (*A*) Variation in triggering rate λ with k_{off} for various KPR sequence lengths m and $M = 10$ peptide-MHC complexes. (*B*) Variation in triggering rate λ with k_{off} for various M and length $m = 7$ fixed. (*C*) Triggering-rate contours $\lambda = 1$, 2, 3, 5, and 10 s^{-1} in the k_{off} –M plane, showing interdependence between these two parameters.

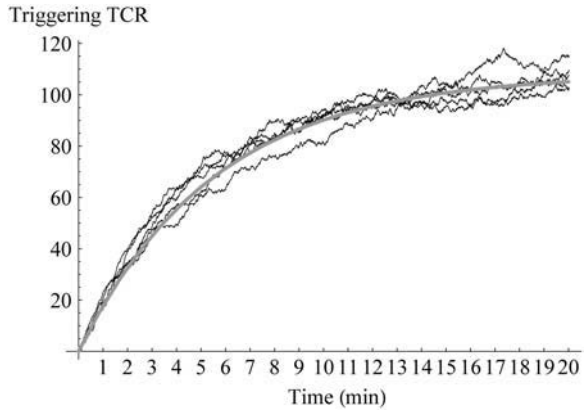

FIGURE 4 Queue trajectories. Three sample paths for the process $T^*(t)$ and the expected trajectory (*shaded line*) for $M = 10$ and $k_{off} = 0.1\ s^{-1}$. The equilibrium value ρ of the number of a triggered TCRs is 108. Paths simulated with a Monte Carlo scheme.

threshold strategies based on low agonist numbers ($M_{total} \leq 10$) are poor at discriminating peptides (Fig. 5) compared to those at higher densities. The primary factor governing specificity is the queue occupancy size, or threshold level, with order $Ca < IS < Cx < Cy$ identical to the specificity order. Factors that increase the threshold improve specificity since the noise is reduced; thus strategies using either higher agonist densities M_{total} or longer time intervals (allowing activated TCRs to accumulate in the queue) have higher specificity. However, because of loss processes from the queue, there is little further improvement after time intervals that exceed 10 min; this is illustrated in Fig. 5 for cytokine secretion ($\tau = 10$ min and $\tau = 3$ h are practically indistinguishable) and Fig. 6 for IS strategy. The limiting factor in specificity improvement is the downregulation rate. Improvements with duration τ arise because the queue size increases, but this saturates as the queue reaches equilibrium, while the expected queue size λ/μ is limited by the downregulation rate μ for any given triggering rate. The optimal strategy is to count the number of triggerings (17), which is effectively achieved by the queue up to $\tau < \mu^{-1}$. Thus, for $\tau \geq 10$ min, a T cell has a tight specificity in k_{off} at low agonist numbers ($M = 10$), which contrasts to the broad response seen at $\tau = 30$ s (Fig. 6 *A*). To sharpen the response further, the downregulation rate would have to be reduced with a time $\tau \sim \mu^{-1}$ achieving near-optimal specificity.

The specificity is in fact higher than can be achieved for the deterministic KPR scheme of Fig. 1. This is because of the use of a threshold. If there was no noise, the range of k_{off} values that trigger a T cell at a given density of agonist would be given by $\lambda(M, k_{off}) > n\mu$ (using steady state for illustration, i.e., a long time-interval τ). This range can be obtained from the contour plot in Fig. 3 *C* by locating the interval in k_{off} between the intersections of the contour and the vertical corresponding to the appropriate M_{total} density. As M increases, the range extends; i.e., poorer agonists can activate the T cell. With noise, these qualities are preserved except that the sharp boundary is smoothed. The extended range in k_{off} with higher M_{total} means that specificity is very sensitive to agonist density (Fig. 5 *C*). The KPR scheme determines specificity degradation with increasing M since the boundaries move as $(dk_{off}/dM)|_{\lambda = n\mu^{-1}}$ along the triggering-rate contour λ.

The kinetic proofreading scheme is essential for high specificity, because triggering-cascades with zero intermediary steps ($m = 0$) have an extremely poor specificity (Fig. 6 *B*), the activation probability for very weak agonists ($k_{off} \sim 1\ s^{-1}$) becoming substantial at $\tau = 30$ s. Extending the time

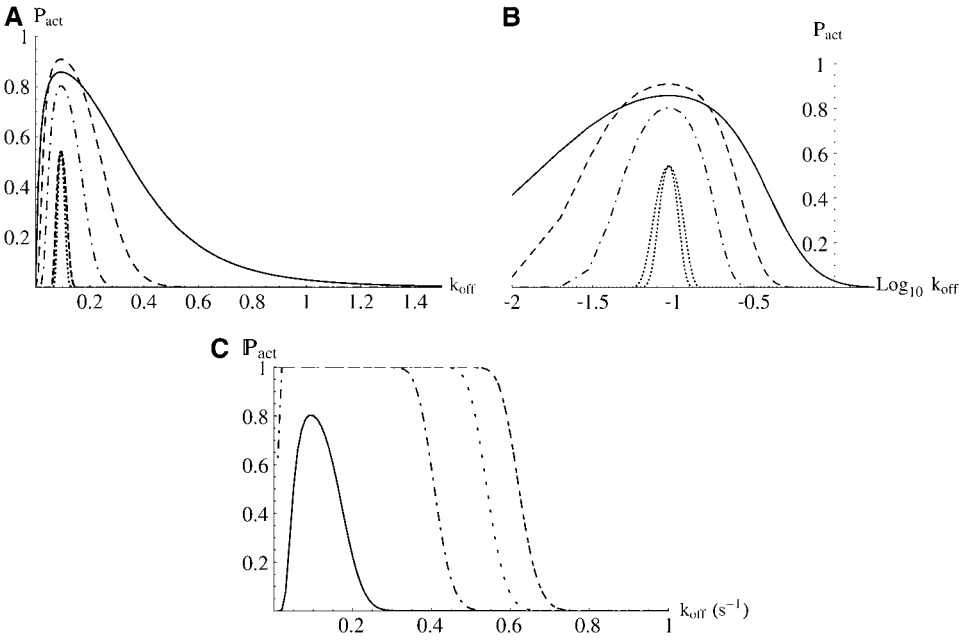

FIGURE 5 Specificity. The response peaks around the optimal k_{off} with varying abilities to filter-out nonspecific agonists. (*A*) Comparison of T-cell activation under threshold conditions of Table 1. Cases are: *Calcium* (*solid*), $\tau =$ 30 s, $\mathbb{P}_{act} = 0.95$, $n = 1$, $M = 2$; *Synapse formation* (*dash*), $\tau = 30$ s, $\mathbb{P}_{act} = 0.9$, $n = 7$, $M = 10$; *Cytotoxicity* (*dot-dash*), $\tau = 10$ min, $\mathbb{P}_{act} = 5/6$, $n =$ 25, $M = 3$; and *Cytokine secretion* (*dotted*), two cases at 10 min and 3 h, $\mathbb{P}_{act} = 0.5$, $M = 100$. (*B*) As panel *A* but with log-scale. (*C*) Cytotoxicity signal at 10 min showing loss of specificity as M increases. $M = 3$ (*solid*) and $M = 10$, 20, 30 (*dot-dashed*, *dotted*, *dashed*). In all cases, $m = 7$ for the KPR scheme.

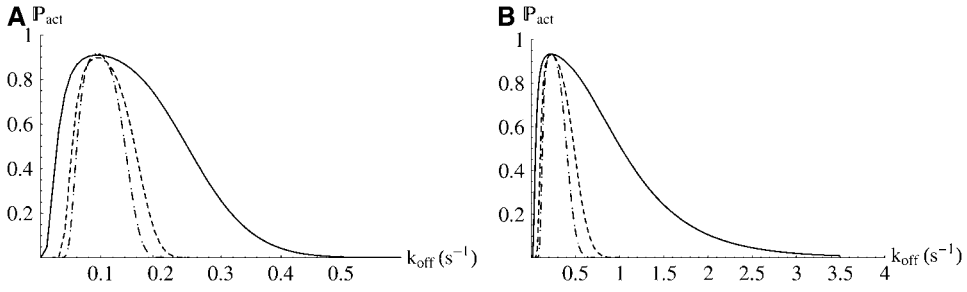

FIGURE 6 Comparison of the immunological synapse (*IS*) threshold strategy for fixed agonist density $M = 10$ at various time points $\tau = 30s$ (*solid*), 10 min (*dash*), and 1 h (*dot-dash*). To compare the response, we set $\mathbb{P}_{act} \approx 0.9$ for each time period under optimal dissociation rate conditions, $(k_{off})_{opt} = 0.1\,s^{-1}$. (*A*) KPR sequence length $m = 7$. For $\tau = 30$ s, the threshold is $n = 7$. When $\tau = 10$ min, $\tau = 1$ h the threshold is raised to $n = 72$ and $n = 108$, respectively. (*B*) The case $m = 0$, i.e., no intermediate activations, showing reduced specificity with respect to panel *A*.

interval to $\tau = 10$ min improves the specificity, but it remains an order-of-magnitude broader than the $m = 7$ KPR sequence.

Sensitivity and background stimulation

Sensitivity of T-cell activation to agonist density is shown in Fig. 7, demonstrating an effectively switchlike behavior for activation with respect to pMHC density M. This behavior is a consequence of the threshold criterion and the linearity of the triggering rate on pMHC density M_{total}. Since poor agonist quality can be compensated by high agonist density to give the same triggering rate (Fig. 3 *C*), it is not surprising that T cells can be activated under a threshold strategy by poor agonists at sufficiently high density; in fact, there is a reasonably modest increase in agonist density from 100 to 150 under a reduction in mean complex lifetime from 10 s to 3 s ($\geq$10 min threshold), while a lifetime of 1 s requires $M > 6400$. This emphasizes the combined effects of half-life and agonist density on specificity; for the cytokine strategy at agonist densities in the range of $100 < M < 125$, we can discriminate $k_{off} = 0.1$ and $0.2\ s^{-1}$, while for $M < 100$ there is no response to either agonist, and for $M > 130$ these agonists cannot be distinguished (Fig. 7). Strategies with higher thresholds perform better at discriminating between good and poor agonists in that a greater absolute increase in pMHC number is required.

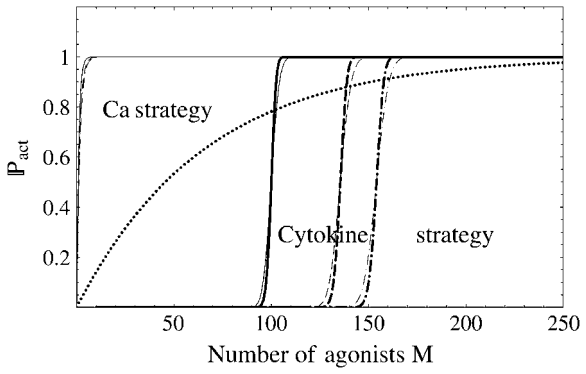

FIGURE 7 Sensitivity. Activation probability $\mathbb{P}_{act}$ as a function of the agonist density M, calcium (Ca), and cytokine secretion (Cy) strategies. A T cell shows a sharp, switchlike behavior in agonist density M, rising sharply over a very narrow range of M. Left set of curves correspond to the calcium threshold, $\tau = 30$ s, right set to the cytokine secretion threshold at $\tau = 10$ min (*thin*) and $\tau = 1$ h (*thick line*). The leftmost curve of each group corresponds to $k_{off} = 0.1\ s^{-1}$ (*solid*), the middle to $0.2\ s^{-1}$ (*dash*) and the rightmost one to $0.03\ s^{-1}$ (*dot-dash*). For the calcium response, the case $k_{off} = 1\ s^{-1}$ is also shown (*dotted*); for the cytokine strategy, this is positioned at $\sim M = 6400$. For each threshold, the optimal agonist with $k_{off} = 0.1\ s^{-1}$ requires the minimal number of agonists to activate.

We observe that for neutral agonists with $k_{off} = 3\ s^{-1}$ (lifetime 0.3 s), pMHC numbers of the order of 10^5 are required to achieve a triggering rate sufficient for activation (cytokine strategy), while 1000 peptides with $k_{off} \sim 1\ s^{-1}$ have a negligible triggering rate. This indicates that background activation can effectively be filtered out provided that self-peptide half-lives are sufficiently small.

Variable agonist density

Only with recent individual pMHC fluorescence studies has the number of pMHC within the contact interface been observed (7). In practice, the number of agonists in the interface is stochastic for a given level of infection, or peptide pulsing. Further, the area of the T cell-APC contact interface does not cover the whole APC surface. We model the number of agonists M as Poisson with mean (and variance) denoted $\bar{M}$. This is appropriate if the area of the contact interface is a fixed proportion of the APC surface, e.g., as may be appropriate in a mature synapse, since the number of pMHC agonists in the interface does not appear to change over time (7). To analyze how the activation probability varies with $\bar{M}$, we compute

$$\mathbb{E}_M[\mathbb{P}_{act}(M)] = \sum_M \mathbb{P}_{act}(M)\exp\{-\bar{M}\}\,\frac{\bar{M}^M}{M!}, \qquad (12)$$

i.e., we weight the activation probability over the distribution in M. Here, $\mathbb{P}_{act}(M) = \mathbb{P}(\tau, \lambda(k_{off}, M), n)$.

Under this stochastic model, the switchlike behavior observed under variation of M is degraded, Poisson noise in M dominating the intrinsic variation in the queue (Fig. 8). The cytokine response in the case $\tau = 10$ min and $\tau = 1$ h are

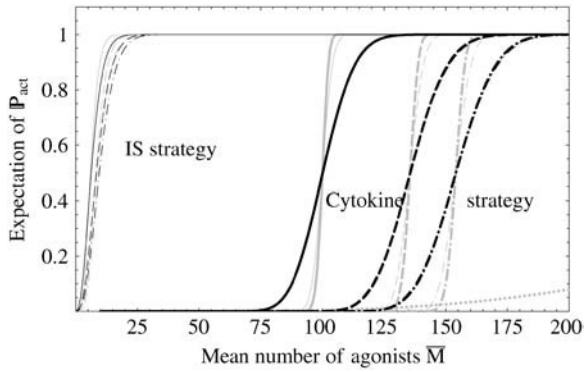

FIGURE 8 Sensitivity with noise. The expected activation probability with agonist density M, IS, and Cy strategies. The responses when there is no noise in the agonist density are shown in gray (Cy as in Fig. 7) and under a Poisson distribution for pMHC density in black (against mean pMHC density). The cases shown are $\tau = 30$ s (IS strategy) on far left, $\tau = 10$ min (*thin line*) and $\tau = 1$ h (*thick line*) for the Cy strategy on right with cases $k_{off} = 0.1$, 0.2, and 0.03 s^{-1} (*solid*, *dashed*, *dash-dot*) as Fig. 7.

almost the same in the presence of noise with a broad response ranging from 75 to 125 in (mean) agonist density in contrast to the range of 90–105 in the nonrandom case ($k_{off} = 0.1$ s^{-1}). Thus, 0.1 s^{-1} and 0.2 s^{-1} are no longer distinguished. This clearly demonstrates that for threshold models the number of triggered TCRs is a good indicator of the actual triggering rate in the interface, i.e., it is both specific and sensitive. However, variation in the number of agonists, and thus the triggering rate, causes a loss of specificity and sensitivity. Achieving control and accurate sampling of the APC surface therefore appears to be a more significant problem than the stochasticity inherent in the queue itself, possibly providing an explanation for the role of the immunological synapse.

Variance in the threshold and time window

The considerations above apply to all the parameters of the system, since they are themselves subject to stochastic fluctuations. For each of the parameters, we can define a tolerance width for the activation probability (for a given peptide lifetime and density) as the length of the parameter range over which the probability $\mathbb{P}_{act}$ rises. As with any probability distribution, the width is quantified by the variance; thus, the total variance is then given to leading order by (assuming parameter variations are independent)

$$var(\mathbb{P}_{act}) = var(\mathbb{P}_{act})|_{\bar{\mathbf{M}},\bar{\tau}..} + var(M)\left(\frac{\partial \mathbb{P}_{act}}{\partial M}|_{\bar{\mathbf{M}},\bar{\tau}..}\right)^2 + var(\tau)\left(\frac{\partial \mathbb{P}_{act}}{\partial \tau}|_{\bar{\mathbf{M}},\bar{\tau}...}\right)^2 + \ldots. \quad (13)$$

Thus, for any parameter, the smaller the *relative tolerance* = *tolerance/mean*, the more sensitive the system is to that parameter. Specifically, if a parameter has a relative error smaller than the relative tolerance-width of the process, its stochasticity is irrelevant, otherwise its stochasticity degrades the detection characteristics of the queue. For agonist density, the relative tolerance of the cytokine strategy was ~1%, and thus the system was very sensitive to variation in agonist numbers (Fig. 8). Tolerance to queue parameters, however, appears more robust with relative tolerances >5% (*cytokine threshold*) for optimal agonists, while the calcium and synapse strategies were very sensitive to the threshold n and period τ (Fig. 9). There remains strong dependence on τ even at 10 min (Fig. 9 *C*), where τ must be in the range 550–650. Under signal competition, e.g., between remaining with the APC versus moving on, an exponential distribution for τ seems justifiable with relative error = 1. Of note, however, is that a hierarchy of thresholds and events reduces this relative error and thus later events such as cytokine secretion may be less constrained by these problems. For variation in the threshold n, the dependence is also strong; for $k_{off} = 0.1$ s^{-1}, the dependence resembles a Poisson distribution (*var* ≈ *mean*). Thus for the synapse threshold, n has a range 7–13 for $0.1 \leq \mathbb{P}_{act} \leq 0.9$, with 50% point at 10, while for the cytokine threshold at 10 min, the corresponding range is of size 30, 50% point at 908. Thus, if there is variation in n that exceeds this range, then $\mathbb{P}_{act}$ as a function of k_{off} and M acquires additional variance—i.e., the dependence on these variables is broader than the queue at fixed τ and n would indicate.

Temporal integration of signals

To analyze time-integrated signals, we integrate over the queue T^* for a period of time τ (hours). We assume the queue is in stationary equilibrium—a good approximation, since the queue equilibrates in time μ^{-1}. If downregulation is included, we integrate over the queue once the T-cell pool size has equilibrated (equilibrium density levels are shown in Fig. 2). This is justified, because the initial transient is short relative to the timescales of integration, and there is often a minimum time of interaction (dead-time) before any cell function is observed.

The integrated signal $a(\tau) = \int_0^\tau T^* dt$ is monotonically increasing in agonist number M and time τ, although with downregulation it saturates in the former at high M (Fig. 10 *A*) but remains linear in τ. It has a maximum in the off-rate close to $k_{off} = 0.1$ s^{-1} (Fig. 10 *B*), a property determined by the underlying kinetic proofreading scheme, since $\mathbb{E}[a(\tau)] = \lambda(M, k_{off})\tau/\mu$. However, as λ saturates at high agonist concentrations, it loses dependence on k_{off} and thus, specificity is degraded. This saturation differs from the threshold model, where saturation was implicit in the threshold mechanism and restricted specificity to a small range of agonist concentrations. The integrated signal also differs substantially from the threshold model in that it is quantitative, and thus there is the additional complication of the variance in the signal. However, this variance is small for time integrations of the order of an hour (Fig. 10 *B*).

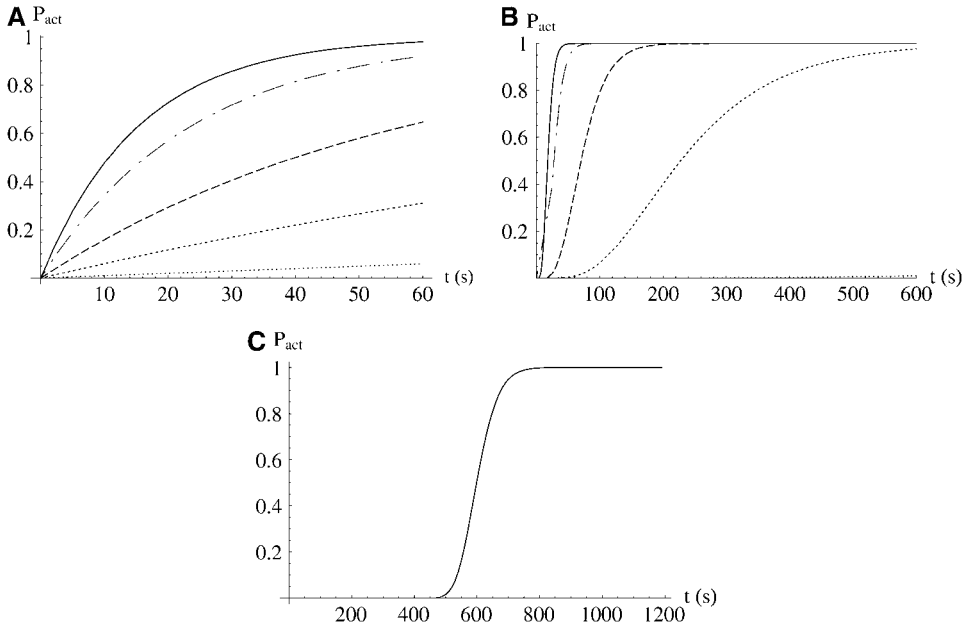

FIGURE 9 Dependence of the threshold model on time interval τ (seconds). (*A*) Calcium (Ca) signal; (*B*) immunological synapse (IS) signal; (*C*) cytokine secretion (Cy) signal at $\tau = 10$ min. Various k_{off} values are shown: $k_{off} = 0.03$ (*dot-dash*), 0.1 (*solid*), 0.4 (*dashed*), 0.6 (*dotted*), and 1.0 (*fine dotted*) s^{-1}. Some curves are close to the axis; for panel *C*, only $k_{off} = 0.1\ s^{-1}$ is visible.

Parameter variation in the queue degraded the specificity of the threshold criteria. However, for the time-integrated signal, the variance associated with triggering and downregulation can be controlled since it contributes to the variance σ^2 (Eq. 9), an argument that is valid provided the time interval of integration is longer than the timescale of any variation in these parameters. Such noise can thus be filtered out by using longer time intervals τ. Cell-to-cell variation, i.e., variation in queue parameters, still remains a problem. Of course, short sampling time intervals τ will have poor specificity; for the queue alone, the relative error is 10%, with time intervals of the order of 10 min (at triggering rates of 0.4 s^{-1}).

CONCLUSION

We analyzed two types of activation processes in the context of a simple linear queue of TCR triggering, specifically threshold models where the number of fully activated TCRs must exceed a threshold n (within a time window τ), and integration of signals from a population of triggered TCRs for a period τ. Our study has shown that both systems can be highly specific and sensitive, and able to filter out background (self-peptide) noise, i.e., can meet both the competing demands of detection of low levels of agonist and discriminate between ligands varying by as little as 30% in their off-rates (49). In fact, threshold models are able to improve on the specificity of the KPR sequence within narrow agonist concentration ranges, but lose specificity as the agonist concentration increases. In contrast, time-integrated signals over the stationary state have a specificity determined by the underlying KPR kinetics, and lose specificity only at very high agonist concentrations through saturation of the triggering rate by processes such as downregulation. For both, specificity improved with the length of the KPR scheme, although under the constraint that sensitivity was preserved (implemented by rescaling k) the effect was large for changes

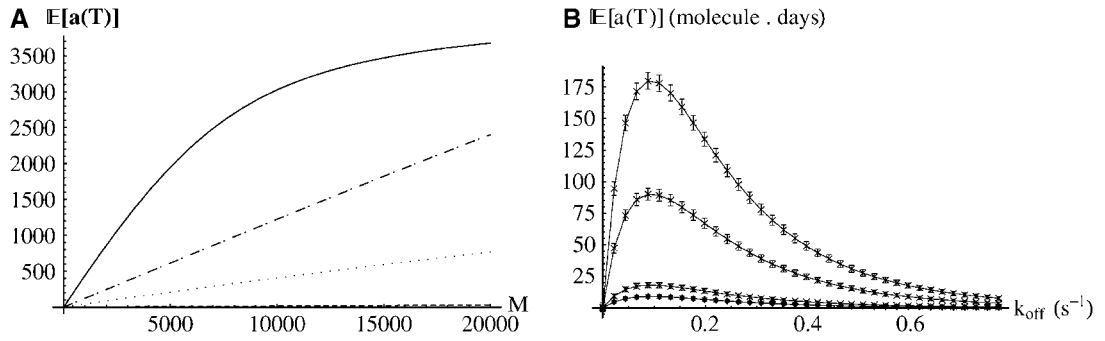

FIGURE 10 Time-integrated signal $\mathbb{E}[a(\tau)]$. (*A*) $\mathbb{E}[a(\tau)]$ as a function of agonist number M for various k_{off}: 0.1 (*solid*), 0.6 (*dot-dash*), 1.4 (*dashed*), and 0.01 (*dotted*) s^{-1}, with $\tau = 1$ h. (*B*) $\mathbb{E}[a(\tau)]$ as a function of k_{off}; various $M = 10, 20, 100$, and 200 with associated standard deviation (*error bars*) for an integration time window $\tau = 1$ h. Units of $\mathbb{E}[a(\tau)]$ are molecule days.

$m = 0$ through to $m = 3$, and thereafter improvement was small. Other models for TCR activation can also be used; for instance, the heterodimer model of activation (50), the triggering rate λ-dependence on M and k_{off} of these models then determining the specificity of the queue and signal-integration models.

System tuning was found to be a significant problem for threshold models, the system parameters need to be tightly controlled for high specificity. In practice, there is likely to be intrinsic variability in the downregulation rate, the threshold level, the time window τ, and KPR kinetics both within a cell (spatial and temporal heterogeneity) and across a clonal population of T cells. Time-integrated signals can control the signal variance by extending the length of the time-integration interval and thus are better estimators of the triggering rate. These results can be understood from consideration of the number of events sampled; time integration increases the number of triggering events sampled as serial triggering of TCRs by peptide-MHC agonists continually report on the presence of the agonist. As the sample size N increases, the relative error of any estimate decreases as $1/N^{1/2}$. Signal integration over the stationary distribution gives a quantitative signal which, once noise levels are low, has a specificity determined by the KPR kinetics and thus the analysis is identical to that of the ordinary differential equation formulation (20,21).

Our study has emphasized a key difference between thresholds set on early and late signals. The specificity improved as the time-interval τ approached $\tau \approx \mu^{-1}$; however, further increase in τ gave little improvement. This is because, for $\tau < \mu^{-1}$, the queue is counting productive triggerings—which is, in fact, an optimal strategy (17). Thresholds set on the rising transient of the signal are thus optimal for that time period, while those at times greater than the half-life of a triggered TCR (μ^{-1}) are monitoring the stationary distribution of the activated TCR population. We also found that of the strategies examined, specificity and sensitivity were inversely correlated; thus strategies with short time intervals and low thresholds were highly sensitive, but had marginal specificity, while strategies on long time intervals and high thresholds were highly specific, but utilized higher levels of agonist. Fundamentally, this implies that in any discussion of specificity the function and conditions must be defined since it is consistent to have both high sensitivity and specificity, as observed for the early calcium signal and late cytokine secretion signal respectively. We predict that, as specificity and sensitivity are further examined for each cell function, this inverse correlation will be realized. In our model we assumed that activated TCRs are downregulated; however, inactivation (dephosphorylation) has also been suggested to occur (41). In the queue model this would increase the rate μ of activated TCRs leaving the queue. This would alter our conclusions in the following respects: the queue would have a lower occupancy and thus high intrinsic noise, and reach steady state faster. Thus, the optimum time for the threshold would decrease below 5 min, while all strategies after that time would have reduced specificity.

T-cell activation is probably a mix of threshold and time-integration signals; for example, a small transient calcium spike is sufficient to activate the transcription factor NFκB but insufficient for NFAT (51). Threshold models have the advantage of speed and thus can be used to prevent extended unproductive APC contacts and quickly locate productive contacts, while their specificity properties are easily saturated with increasing agonist. This suggests that thresholds are predominantly used to establish conditions for efficient signal integration and to determine when signal integration occurs. Cell spreading, adhesion upregulation, cell reorientation, and possibly synapse formation are thus early prerequisite events for the formation of a stable surface contact with the APC, which we hypothesize are controlled by thresholds. Adaptation of these thresholds to the current conditions also allows T cells to reorient toward higher stimulus APCs (31,52), while transient interactions (13) could be controlled by threshold events to optimize high-quality interactions and orchestrate signal integration over a series of contacts—a series of sequential APC conjugations that could partially accommodate for variation between APCs. Signal integration on the scale of hours is more robust to system noise and retains specificity over a range of agonist concentrations. However, signal integration also allows for quantitative responses, relative degrees of activation being observed in T cells, which underpins competition and selection (53–57). The mechanism for this selection is probably the quantitative correlation of stimulus with receptors such as the IL2 receptor (12,29). This contrasts to the innate immune system where maturation and selection do not occur; NK cells, for instance, have been proposed to be regulated by a series of checkpoints (31). We have also commented that high levels of weak agonists and low levels of good agonists can have identical triggering rates. Experimentally it is known that antagonists can deliver negative or inactivation signals (37), thus indicating that the TCR is capable of encoding agonist quality. This may involve signaling from partially activated complexes, which would have a higher representation under shorter lifetime pMHC-TCR complexes, i.e., weak agonists. These negative signals appear to enhance negative feedback paths, but have different effects on different functions; specifically, proliferation was inhibited but not cytotoxicity (58), suggesting negative feedback works on long timescales. Agonist quality k_{off} and agonist density M_{total} may therefore be separated during signal integration while thresholds register only minimal stimulation requirements. Thus, multilayered signaling involving threshold signals and signal integration provide a flexible basis on which to deliver T-cell function, firstly to filter out background levels of self-peptide signaling, and secondly to allow optimal T cells to be selected in an immune response based on agonist detection efficiency.

Experimentally there are key signatures for threshold regulation and signal integration. Thresholds only have a

discrete (ON/OFF) output, or two distinct states, while signal integration can deliver relative or partial degrees of activation. Thus, for cell polarization and cytotoxicity, which are discrete events, thresholds seem very likely. Of interest, however, is whether the threshold is on the triggering rate (λ), triggered TCR density (T^*), or another downstream integrated variable. Integrated signals have a quantitative output that increases with antigen exposure, exposure incorporating the two aspects of duration length and stimulus strength, both of which should be tested since a threshold mechanism may underpin the signal integration. Specifically integrated outputs $a = \int T^*(t)dt$ and $b = time\ when\ T^* > \theta$ both show a correlation with stimulus duration; however, only a has a correlation with stimulus strength (provided T^* remains above threshold θ). Thus, although cytokine production increases with the duration of antigen exposure (8), it is unclear if cytokine output is also proportional to levels of T^*, and over what range, i.e., whether integration is through a quantitative dependence such as a or b. This would require different stimulus levels to be analyzed. The complication is that at a population level, variation of thresholds between cells or signal fluctuations can give output b, or threshold switching more generally, the appearance of a continuous dependence on stimulus strength (or T^*) through a change in the number of cells responding at any one time. This can be addressed through enrichment of subpopulations to remove cell heterogeneity, e.g., sorting on TCR density, or through single-cell experiments. Analysis of the dynamics of molecular circuits and monitoring circuit variables is becoming increasingly possible with noninvasive fluorescent techniques and can potentially distinguish these regulatory mechanisms through a correlation analysis, comparing output (activation) with different variables and their histories (integrations). Experimentally different histories, before activation, would need to be established—such as using antigen exposure intervals with different levels of antigen. For example, single-cell monitoring of NFκB nucleus levels would indicate if NFκB nucleus levels are a better correlate of cytokine output than antigen exposure, or their integrated analogs. Thus, through a manipulation of antigen exposure profiles (strength and duration) and observation of the activation and relaxation kinetics of signal mediators, the particular dependencies of a cell response can be ascertained, and thereby identify where in a regulatory circuit thresholds are set and the mechanism underlying that threshold (e.g., negative feedback). Ultimately, all threshold and signal integration strategies must have a molecular circuit framework.

PARAMETERS

The model has five parameters. The surface density of TCR is taken to be 30,000 (14), i.e., a surface density 100 μm^{-2}, assuming a cell surface of 300 μm^2. The downregulation rate $\mu (= \mu_d)$ is taken as 0.003 s^{-1}, which is the order of magnitude estimated across a variety of studies (46,59). For instance, after 7–15 min, 50% of the TCR are downregulated at 20 μM peptide (estimated to be 9000 pMHC) (14). At this density, within 1 min the majority of the receptors are activated, thus the downregulation curve follows $\exp(-rt)$. This gives $r \sim 0.001\ s^{-1}$, and each activated receptor stays around for 5–10 min. The loss rate of TCRs from the surface is taken as $\mu_0 = 0.01\ min^{-1} = 0.00017\ s^{-1}$, estimated from the secretion inhibition studies, 30% of the surface TCR is lost in 15 min under primaquine treatment (45).

For the TCR/pMHC kinetics, we take a two-dimensional affinity of 20 molecules per μm^2 for an optimal agonist (as measured for CD2-CD48 interaction, which has similar three-dimensional affinities to the TCR/pMHC interaction) (60). An optimal agonist has an off-rate $(k_{off})_{optimal} = 0.1\ s^{-1}$ (48).

REFERENCES

1. Dustin, M. L., T. G. Bivona, and M. R. Philips. 2004. Membranes as messengers in T-cell adhesion signaling. *Nat. Immunol.* 5:363–372.
2. Bossi, G., C. Trambas, S. Booth, R. Clark, J. Stinchcombe, and G. M. Griffiths. 2002. The secretory synapse: the secrets of a serial killer. *Immunol. Rev.* 189:152–160.
3. Hemmer, B., I. Stefanova, M. Vergelli, R. N. Germain, and R. Martin. 1998. Relationships among TCR ligand potency, thresholds for effector function elicitation, and the quality of early signaling events in human T cells. *J. Immunol.* 160:5807–5814.
4. Itoh, Y., and R. N. Germain. 1997. Single cell analysis reveals regulated hierarchical T-cell antigen receptor signalling thresholds and intraclonal heterogeneity for individual cytokine responses of $CD4^+$ T cells. *J. Exp. Med.* 186:757–766.
5. Valitutti, S., S. Muller, M. Dessing, and A. Lanzavecchia. 1996. Different responses are elicited in cytotoxic T lymphocytes by different levels of T-cell receptor occupancy. *J. Exp. Med.* 183:1917–1921.
6. Lezzi, G., K. Karjalainen, and A. Lanzavecchia. 1998. The duration of antigenic stimulation determines the fate of naive and effector T cells. *Immunity.* 8:89–95.
7. Purbhoo, M. A., D. J. Irvine, J. B. Huppa, and M. M. Davis. 2004. T-cell killing does not require the formation of a stable mature immunological synapse. *Nat. Immunol.* 5:524–530.
8. Faroudi, M., R. Zaru, P. Paulet, S. Müller, and S. Valitutti. 2003. Cutting edge: T Lymphocyte activation by repeated immunological synapse formation and intermittent signaling. *J. Immunol.* 171:1128–1132.
9. Huppa, J. B., M. Gleimer, C. Sumen, and M. M. Davis. 2003. Continuous T-cell receptor signaling required for synapse maintenance and full effector function. *Nat. Immunol.* 4:749–755.
10. Gett, A. V., F. Sallusto, A. Lanzavecchia, and J. Geginat. 2003. T-cell fitness determined by signal strength. *Nat. Immunol.* 4:355–360.
11. van Stipdonk, M. J. B., G. Hardenberg, M. S. Bijker, E. E. Lemmens, N. M. Droin, D. R. Green, and S. P. Schoenberger. 2003. Dynamic programming of $CD8^+$ lymphocyte response. *Nat. Immunol.* 4:361–365.
12. Schrum, A. G., and L. A. Turka. 2002. The proliferative capacity of individual naive $CD4^+$ T cells is amplified by prolonged T-cell antigen receptor triggering. *J. Exp. Med.* 196:793–803.
13. Gunzer, M., A. Schafer, S. Borgmann, S. Gragge, K. S. Zanker, E. B. Brocker, E. Kampgen, and P. Friedl. 2000. Antigen presentation in extracellular matrix: interactions of T cells with dendritic cells are dynamic, short lived, and sequential. *Immunity.* 13:323–332.
14. Valitutti, S., S. Muller, M. Cella, E. Padovan, and A. Lanzavecchi. 1995. Serial triggering of many T-cell receptors by a few peptide-MHC complexes. *Nature.* 375:148–151.

15. Chan, C., A. J. T. George, and J. Stark. 2001. Cooperative enhancement of specificity in a lattice of T-cell receptors. *Proc. Natl. Acad. Sci. USA*. 98:5758–5763.

16. Chan, C., J. Stark, and A. J. T. George. 2004. Feedback control of T-cell receptor activation. *Proc. Roy. Soc. Biol.* 271:931–939.

17. Noest, A. 2000. Designing lymphocyte functional structure for optimal signal detection: *voila*, T cells. *J. Theor. Biol.* 207:195–216.

18. van den Berg, H. A., D. A. Rand, and N. J. Burroughs. 2001. A reliable and safe T-cell repertoire based on low-affinity T-cell receptors. *J. Theor. Biol.* 209:465–486.

19. Lee, K.-H., A. R. Dinner, C. Tu, G. Campi, S. Raychaudhuri, R. Varma, T. N. Sims, W. R. Burack, H. Wu, J. Wang, O. Kanagawa, M. Markiewicz, P. M. Allen, M. L. Dustin, A. K. Chakraborty, and A. S. Shaw. 2003. The immunological synapse balances T-cell receptor signaling and degradation. *Science*. 302:1218–1222.

20. T. W. McKeithan. 1995. Kinetic proofreading in T-cell receptor signal transduction. *Proc. Natl. Acad. Sci. USA*. 92:5042–5046.

21. Rabinowitz, J. D., C. Beeson, D. S. Lyons, M. M. Davis, and H. M. McConnell. 1996. Kinetic discrimination in T-cell activation. *Proc. Natl. Acad. Sci. USA*. 93:1401–1405.

22. Chan, C., A. J. T. George, and J. Stark. 2003. T-cell sensitivity and specificity—kinetic proofreading revisited. *Discr. Contin. Dynam. Sys. B*. 3:343–360.

23. Stefanova, I., B. Hemmer, M. Vergelli, R. Martin, W. E. Biddison, and R. N. Germain. 2003. TCR ligand discrimination is enforced by competing ERK positive and SHP-1 negative feedback pathways. *Nat. Immunol.* 4:248–254.

24. Veillette, A., S. Latour, and D. Davidson. 2002. Negative regulation of immunoreceptor signaling. *Annu. Rev. Immunol.* 20:669–707.

25. Faeder, J. R., W. S. Hlavacek, I. Reischl, M. L. Blinov, H. Metzger, A. Redondo, C. Wofsy, and B. Goldstein. 2003. Investigation of early events in FCε RI-mediated signaling using a detailed mathematical model. *J. Immunol.* 170:3769–3781.

26. Irvine, D. J., M. A. Purbhoo, M. Krogsgaard, and M. M. Davis. 2002. Direct observation of ligand recognition by T cells. *Nature*. 419:845–849.

27. Revy, P., M. Sospedra, B. Barbour, and A. Trautmann. 2001. Functional antigen-independent synapses formed between T cells and dendritic cells. *Nat. Immunol.* 2:925–931.

28. Weiss, A., R. Shields, M. Newton, B. Manger, and J. Imboden. 1987. Ligand-receptor interactions required for commitment to the activation of the Interleukin-2 gene. *J. Immunol.* 138:2169–2176.

29. Iezzi, G., K. Karjalainen, and A. Lanzavecchia. 1998. The duration of antigenic stimulation determines the fate of naive and effector T cells. *Immunity*. 8:89–95.

30. Schwarzmann, N., S. Kunerth, K. Weber, G. W. Mayr, and A. H. Guse. 2002. Knock-down of the Type-3 ryanodine receptor impairs sustained Ca^{2+} signaling via the T-cell receptor/CD3 complex. *J. Biol. Chem.* 277:50636–50642.

31. Wulfing, C., B. Purtic, J. Klem, and J. D. Schatzle. 2003. Stepwise cytoskeletal polarization as a series of checkpoints in innate but not adaptive cytolytic killing. *Proc. Natl. Acad. Sci. USA*. 100:7767–7772.

32. van der Merwe, A. P., S. J. Davis, A. S. Shaw, and M. L. Dustin. 2000. Cytoskeletal polarisation and redistribution of cell-surface molecules during T-cell antigen recognition. *Semin. Immunol.* 12: 5–21.

33. Krummel, M., M. D. Sjaastad, C. Wülfing, and M. M. Davis. 2000. Differential clustering of CD4 and CD3ζ during T-cell recognition. *Science*. 289:1349–1352.

34. Freiberg, B. A., H. Kupfer, W. Maslanik, J. Delli, J. Kappler, D. M. Zaller, and A. Kupfer. 2002. Staging and resetting T-cell activation in SMACs. *Nat. Immunol.* 3:911–917.

35. Hoffmann, A., A. Levchenko, M. L. Scott, and D. Baltimore. 2002. The IκB-NF-κB signalling module: temporal control and selective gene activation. *Science*. 298:1241–1245.

36. Lewis, R. S. 2003. Calcium oscillations in T-cells: mechanisms and consequences for gene expression. *Biochem. Soc. Trans.* 31:925–929.

37. Dittel, B. N., I. Stefanova, R. N. Germain, and C. A. Janeway. 1999. Cross-antagonism of a T-cell clone expressing two distinct T-cell receptors. *Immunity*. 11:289–298.

38. Dustin, M. L. 2004. Stop-and-go traffic to tune T-cell responses. *Immunity*. 21:305–314.

39. Hopfield, J. J. 1974. Kinetic proofreading: a new mechanism for reducing errors in biosynthetic processes requiring high specificity. *Proc. Natl. Acad. Sci. USA*. 71:4135–4139.

40. Werlen, G., and E. Palmer. 2002. The TCR signalosome: a dynamic structure with expanding complexity. *Curr. Opin. Immunol.* 14:299–305.

41. Coombs, D., A. M. Kalergis, S. G. Nathenson, C. Wofsy, and B. Goldstein. 2002. Activated TCRs remain marked for internalisation after dissociation from pMHC. *Nat. Immunol.* 3:926–931.

42. Grakoui, A., S. K. Bromley, C. Sumen, M. M. Davis, A. S. Shaw, P. M. Allen, and M. L. Dustin. 1999. The immunological synapse: a molecular machine controlling T-cell activation. *Science*. 285: 221–227.

43. Li, Q.-J., A. R. Dinner, S. Qi, D. J. Irvine, J. B. Huppa, M. M. Davis, and A. K. Chakraborty. 2004. CD4 enhances T-cell sensitivity to antigen by coordinating Lck accumulation at the immunological synapse. *Nat. Immunol.* 8:791–799.

44. Liu, H. Y., M. Rhodes, D. L. Wiest, and D. A. A. Vignali. 2000. On the dynamics of TCR:CD3 complex cell surface expression and down-modulation. *Immunity*. 13:665–675.

45. Das, V., B. Nal, A. Dujeancourt, M. I. Thoulouze, T. Galli, P. Roux, A. Dautry-Varsat, and A. Alcover. 2004. Activation-induced polarized recycling targets T-cell antigen receptors to the immunological synapse: involvement of SNARE complexes. *Immunity*. 20:577–588.

46. Sousa, J., and J. Carneiro. 2000. A mathematical analysis of TCR serial triggering and down-regulation. *Eur. J. Immunol.* 30:3219–3227.

47. Lollo, B. A., K. W. H. Chan, E. M. Hanson, V. T. Moy, and A. A. Brian. 1993. Direct evidence for two affinity states for lymphocyte function-associated antigen 1 on activated T cells. *J. Biol. Chem.* 268:21693–21700.

48. Lyons, D. S., S. A. Lieberman, J. Hampl, J. Boniface, Y. Chien, L. J. Berg, and M. M. Davis. 1996. A TCR binds to antagonist ligands with lower affinities and faster dissociation rates than to agonists. *Immunity*. 5:53–61.

49. Kersh, G. J., M. J. Miley, C. A. Nelson, A. Grakoui, S. Horvath, D. L. Donermeyer, J. Kappler, P. M. Allen, and D. H. Fremont. 1998. Structural and functional consequences of altering a peptide MHC anchor residue. *J. Immunol.* 166:3345–3354.

50. Krogsgaard, M., Q. J. Li, C. Sumen, J. B. Huppa, M. Huse, and M. M. Davis. 2005. Agonist/endogenous peptide-MHC heterodimers drive T-cell activation and sensitivity. *Nature*. 434:238–243.

51. Randriamampita, C., and A. Trautmann. 2004. Ca^{2+} signals and T lymphocytes ''new mechanisms and functions in Ca^{2+} signalling''. *Biol. Cell*. 96:69–78.

52. Valitutti, S., S. Muller, M. Dessing, and A. Lanzavecchi. 1996. Signal extinction and T-cell repolarization in T helper cell-antigen-presenting cell conjugates. *Eur. J. Immunol.* 26:2012–2016.

53. van Bergen, J., Y. Kooy, and F. Koning. 2001. CD4-independent T cells impair TCR triggering of CD4-dependent T cells: a putative mechanism for T-cell affinity maturation. *Eur. J. Immunol.* 31:646–652.

54. Dummer, W., B. Ernst, E. LeRoy, D.-S. Lee, and C. D. Surh. 2001. Autologous regulation of naive T-cell homeostasis within the T-cell compartment. *J. Immunol.* 166:2460–2468.

55. Schluns, K. S., W. C. Kieper, S. C. Jameson, and L. Lefrancois. 2000. Interleukin-7 mediates the homeostasis of naive and memory CD8 T cells *in vivo*. *Nat. Immunol.* 1:426–432.

56. Kedl, R. M., W. A. Rees, D. A. Hildeman, B. C. Schaefer, T. Mitchell, J. W. Kappler, and P. Marrack. 2000. T cells compete for access to antigen-bearing antigen-presenting cells. *J. Exp. Med.* 192:1105–1113.

57. Rees, W., J. Bender, T. K. Teague, R. M. Kedl, F. Crawford, P. Marrack, and J. Kappler. 1999. An inverse relationship between T-cell receptor affinity and antigen dose during $CD4^+$ T-cell responses in vivo and in vitro. *Proc. Natl. Acad. Sci. USA.* 96:9781–9786.

58. Yang, W., and H. M. Grey. 2003. Study of the mechanism of TCR antagonism using dual-TCR-expressing T cells. *J. Immunol.* 170:4532–4538.

59. Wofsy, C., D. Coombs, and B. Goldstein. 2001. Calculations show substantial serial engagement of T-cell receptors. *Biophys. J.* 80:606–612.

60. Dustin, M. L., D. E. Golan, D. M. Zhu, J. M. Miller, W. Meier, E. A. Davies, and P. A. van der Merwe. 1997. Low affinity interaction of human or rat T-cell adhesion molecule CD2 with its ligand aligns adhering membranes to achieve high physiological affinity. *J. Biol. Chem.* 272:30889–30898.